

https://dspace.org/

The effect of trees on physical and chemical properties of substrata contaminated by gold mine waste disposal

Arendze, Shakera

2015
http://hdl.handle.net/10539/18548

Downloaded from a DSpace repository. https://dspace.org/

THE EFFECT OF TREES ON PHYSICAL AND CHEMICAL PROPERTIES OF SUBSTRATA CONTAMINATED BY GOLD MINE WASTE DISPOSAL

Shakera Arendze

0200020P

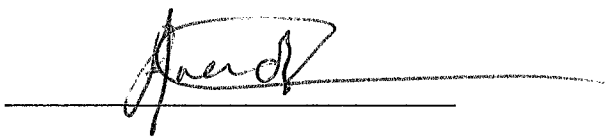
A Research Report submitted to the Faculty of Science, University of the Witwatersrand, Johannesburg, in partial fulfilment of the requirements for the Degree of Master of Science.

Johannesburg,South Africa

2015

DECLARATION

I declare that this Research Report is my own, unaided work. It is being submitted for the Degree of Master of Science at the University of the Witwatersrand, Johannesburg. It has not been submitted before for any degree or examination at any other University.



Signature of Candidate

Signed on 22 day of May 2015 in Johannesburg.

ABSTRACT

The Witwatersrand Basin has the world's richest deposits of gold and low-grade uranium, with South Africa being the world's leading producer of gold. In South Africa, 70% of all waste is generated by mining, mainly the gold and uranium, platinum and coal sectors. In the Witwatersrand Basin alone, there is approximately 400 km^2 of gold tailings storage facilities (TSFs) and footprints. Acid rock drainage (ARD) is one of the most severe types of mine pollution and emanates from ore being exposed to both oxygen and water, which acidifies the water leaching through the dumps. This could potentially percolate into ground water systems, and eventually river systems. ARD could lead to contamination by metals and metalloids and could affect the chemical speciation of these elements.

Phytoremediation involves using plants and soil micro flora, as well as non-living biomass to improve the quality of a substrate; as plants naturally take up metals from soil and water. Metal hyperaccumulators are of interest as they are capable of accumulating high concentrations of metals and metalloids in their tissues, thus making them highly applicable for mine remediation purposes.

The aim of the project was to assess whether two species of trees, namely *Rhus lancea* and *Tamarix usneoides*, have the potential to phytoremediate ARD by modifying the physical and chemical properties in the substrate, versus a control. For each tree species, two treatments, i.e. woodland and grassland (control) substrates were studied within two gold mine sites near Klerksdorp (on the western part of the basin), with different soil forms and conditions for the growth of trees. The results were interpreted in order to assess if either of these tree species show potential for remediation of ARD-impacted substrata.

Soil samples were collected from the two gold mine sites in the dry season of 2009. Physical analysis of the soil samples included: soil colour; carbon, hydrogen,

nitrogen and sulphur (CHNS) analysis, X-ray fluorescence (XRF); soil fertility; and soil texture of the soil samples. Chemical analysis included the initial physical-chemical soil solution measurements, the sequential extraction of the soil using the European Communities Bureau of Reference (BCR) method, and the analysis of the BCR extracts using inductively coupled plasma - optical emission spectroscopy (ICP-OES). Analysis was done for the following major nutrients: calcium, magnesium, potassium, phosphorous and sulphur, and trace elements: aluminium, arsenic, chromium, copper, iron, lead, manganese, mercury, nickel, titanium, uranium, vanadium and zinc. The statistical analysis included: descriptive statistics, percentage differences, principal components analysis (PCA), histograms, analysis of variance (ANOVA), and linear regression analysis (LRA).

The trees enhanced the physical-chemical characteristics of the soil, i.e. the pH increased by 7% due to alkalinising effects; the conductivity increased by 88% due to salt and metal hyperaccumulation from the soil; and the redox potential decreased by 15%, thus reducing the oxidation potential of the soil.

The trees also improved the phyical soil characteristics improving soil texture, due to the introduction of finer particles into the soil; i.e 18% more clay particles.

The chemical condition of the soil in the presence of the trees also bettered, as the concentration of calcium increased by 14% in the soil due to top-soil enrichment. Hence the trees have enriched the soil substrate by increasing the calcium in the soil. PCA showed that calcium, magnesium and sulphur were grouped together while phosphorous and potassium formed another grouping; indicating similar behaviour within each major nutrient group. ANOVA results suggested that the concentration of the major nutrients showed no significant difference between the woodland and the grassland treatment substrates (p = 0.388 for the first grouping and p = 0.405 for the second grouping). The linear regression results indicated that the major nutrients had a significant, linear, negative relationship with depth; hence the equation which was generated could be used in future predictions.

Nickel decreased in the presence of the trees by between 39%. The trees likely absorbed the nickel ions from the soil, causing a decrease in the soil solution.

The PCA showed three distinct groupings, namely one for mercury, vanadium, chromium, arsenic, titanium, nickel and zinc; another for aluminium, manganese, and iron; and lastly uranium and lead formed another grouping, again indicating similar behaviour in each grouping. The ANOVA results indicated that aluminium, manganese and iron showed a significant difference between the woodland and the grassland treatment substrates ($p = 0.00$), and no significant difference for the other trace elements ($p = 0.40$ and $p = 0.20$). The linear regression data indicated uranium and lead had a significant, quadratic correlation with depth ($p = 0.01$), while the other trace elements did not have a significant correlation with depth.

Distribution curves showed that aluminium, chromium, iron, phosphorous, potassium, titanium, vanadium and nickel (at the VRMP), were mainly present in the residual fraction, while calcium, magnesium, manganese and nickel (at the VRWC) were mainly present in the BCR fractions. The trees did not change the percentage distribution of aluminium, chromium, iron, phosphorous, potassium, titanium, vanadium and nickel (at the VRMP), but did change that of calcium, magnesium, manganese and nickel (at the VRWC)

The study revealed that *Rhus lancea* and *Tamarix usneoides* tree species have a great apititude for the treatment of ARD through phytoremediation, as the physical, and chemical characteristics of the mine soils improved in the presence of the trees.

The research also highlighted the differences between the sites, and it was found that the overall soil quality was better at the VRWC than at the VRMP. For example the conductivity of the soil was 168% higher, the CEC in terms of soil fertility was 129% higher, and all major nutrients were between 96% and 183% higher at the VRWC than at the VRMP.

Differences between the tree species, i.e. *Tamarix usneoides* and *Rhus lancea* were also investigated, and it was found that *Tamarix usneoides* was more effective in improving the overall quality of the soil. For example the buffer pH was 10% higher, and the conductivity 107% higher in the soil surrounding *Tamarix usneoides*, while the redox potential was 18% lower, thus improving some of the conditions which exacerbate ARD. The magnesium was 71% in the presence of *Tamarix usneoides*.

DEDICATION

My loving and supportive parents

Faried and Nazley Arendze

You have guided me well

My beloved cousin

Candice Trompetter Moon

In memory of your amazing spirit

ACKNOWLEDGEMENTS

In the name of Allah, The Most Gracious, The Most Merciful. All praise and thanks are due to Allah for the giving me the strength to complete this project. Ameen.

I would like to thank my supervisor Dr Hlanganani Tutu for his help, guidance, support, encouragement, and patience in helping me finish my project. His presence and direction during my project was priceless and I appreciate every moment that was spent helping me.

Ms Isabel Weiersbye thank you for the support and for recruiting me into the Ecological Engineering and Phytoremediation Programme. It was an interesting and relevant project to be part of considering the AMD issue in South Africa.

Thank you to AngloGold Ashanti for funding both the project and my studies.

Prof Ewa Cukrowska and the rest of the Environmental Analytical Chemistry research group for their help and support.

David Furniss, Sashnee Raja, Sheena Kennedy, Mark Cooper, Herman Du Preez, Jenny Botha, Thendo Nethengwe, Lindokuhle Hlongwane, and Macdonald Wanenge for all their assistance throughout my project.

Taimos Mavunganidze and Thuthuka Mabaso for their technical assistance and guidance in the laboratory.

Thank you to my family, friends and work colleagues for their support.

Jazak-Allah Khair to my parents, Faried and Nazley Arendze, for their love and guidance through not only this project but everything else in my life. I am blessed to have you both in my life.

Jazak-Allah Khair to my brother, Ziyaad Arendze, for his encouragement and for being a great role model.

Lastly Jazak-Allah Khair to Mohamed Jooma, for his dedication, help, patience, love and support through the project.

CONTENTS **PAGE**

DECLARATION ii

ABSTRACT iii

DEDICATION viii

ACKNOWLEDGEMENTS ix

LIST OF FIGURES xiv

LIST OF TABLES xxi

LIST OF ABBREVIATIONS xxiv

LIST OF SYMBOLS xxvi

CHAPTER ONE - INTRODUCTION **1**

1.1 Mining and mine pollution on the Witwatersrand 1

1.2 Mine pollution remediation 7

CHAPTER TWO - LITERATURE REVIEW **11**

2.1 Chemical speciation and metal mobility 11

2.2 Phytoremediation and metal hyperaccumulation in plants 12

CHAPTER THREE – MOTIVATION **16**

3.1 Aims and objectives 16

3.2 Hypotheses 17

CHAPTER FOUR - ANALYTICAL TECHNIQUES **18**

4.1 ICP-OES 18

4.2 CHNS Elemental analysis 19

4.3 XRF Spectroscopy 21

CHAPTER FIVE – METHODOLOGY **24**

5.1 Experimental design 24

5.1.1 The study area 24

5.1.2 The tree species 28

5.1.3 Experimental design 31

5.2 Sample collection 32

5.3 Sample preparation 33

5.4 Analyses of soil samples 36

5.4.1 Chemical analysis 36

5.4.2 Physical analysis 40

5.5 Certified reference material 48

5.5 Statistical analysis 50

CHAPTER SIX – INITIAL SOIL ANALYSIS **54**

6.1 Soil colour 54

6.2 Physical-chemical soil solution measurements 55

6.3 Statistical analysis 61

6.3 Summary and conclusions 66

CHAPTER SEVEN – PHYSICAL SOIL ANALYSIS **69**

7.1 Soil Texture 69

7.1.1 Soil class 69

7.1.2 Statistical analysis 72

7.2 Soil Fertility 75

7.2.1 Cation exchange capacity 75

7.2.2 Organic carbon 77

7.2.3 Primary nutrients 79

7.2.4 Secondary nutrients 82

7.2.5 Statistical analysis 85

7.3 CHNS analysis 88

7.3.1 Elemental ratios 88

7.3.2 Statistical analysis 90

7.4 Summary and Conclusions 93

7.4.1 Soil texture 94

7.4.2 Soil fertility 95

7.4.3 CHNS analysis 95

CHAPTER EIGHT - SEQUENTIAL EXTRACTION RESULTS **97**

8.1 Major nutrients 97

8.1.1 BCR extraction curves 97

8.1.2 Statistical analysis 105

8.2 Trace elements 112

8.2.1 BCR extraction curves 112

8.2.2 Statistical analysis 132

8.3 Distribution curves 142

8.4 Summary and Conclusions 147

8.4.1 Major nutrients 147

8.4.2 Trace elements 150

8.3.3 Distribution curves 153

CHAPTER NINE - SUMMARY AND CONCLUSIONS 154

10.1 The potential of the trees for acid rock drainage remediation 154

10.2 Differences between the Vaal River sites 156

10.3 Differences between the tree species 157

10 REFERENCES 159

11 APPENDICES 167

Appendix A – Soil Photos 167

Appendix B – CRM reference sheet 176

Appendix C – Data from Statistical Analysis 187

LIST OF FIGURES

Figure 1.1 Layout of the Witwatersrand basin, with the mining regions in an arc from East-West (Weiersbye *et al.*, 2006)

Figure 1.2 A conceptual model of acid rock drainage in the Witwatersrand region (Tutu *et al.*, 2008)

Figure 1.3 Source control options to minimise or prevent the generation of acid rock drainage (Johnson, 2005)

Figure 1.4 Migration control options to remediate acid rock drainage waters (Johnson, 2005)

Figure 2.1 Eh-pH diagram for Uranium species in high sulphate acid mine surface water (Tutu *et al.*, 2008)

Figure 4.1 Schematic diagrams representing the atomic emission process

Figure 4.2 A schematic diagram of the setup of an energy dispersive spectrometer (Khalid *et al.*, 2011)

Figure 5.1 Location of the trials within the Witwatersrand Basin

Figure 5.2 An aerial photo of the Vaal River mining operation near Klerksdorp

Figure 5.3 The layout of the woodland trials at the Vaal River West Complex site

Figure 5.4 The layout of the woodland trials at the Vaal River Mispah site

Figure 5.5 Groundwater plumes at the VRWC TSF (AGA Groundwater report, 2007)

Figure 5.6 Groundwater plumes at the VRMP TSF (AGA Groundwater report, 2007)

Figure 5.7 A picture of 4-year old *Rhus lancea* trees at the VRWC

Figure 5.8 A picture of 4-year old *Tamarix usneoides* trees at the VRMP

Figure 5.9 A scanning electron micrograph of salt crystals on *Tamarix* usneoides foliar glands (Weiersbye, unpublished)

Figure 5.10 A picture showing how the soil core samples were collected in the rooting zone

Figure 5.11 A flow diagram showing sample preparation for soil core samples from point of collection

Figure 5.12 A flow diagram showing sample preparation and sample analysis schemes for soil core samples from point of collection

Figure 5.13 A typical BCR sequential extraction curve for Mn in sediments of a mine pan (Cukrowska *et al.*, 2006)

Figure 5.14 The soil texture triangle representing the various soil texture classes (FAO/IIASA/ISRIC/ISS-CAS/JRC, 2009)

Figure 6.1 A control soil core sample taken at the Vaal River West Complex.

Figure 6.2 A control soil core sample taken at the Vaal River Mispah.

Figure 6.3 pH results with depth for soil at the Vaal River West Complex

Figure 6.4 pH in 0.1 M KCl results with depth for soil at the Vaal River West Complex

Figure 6.5 pH results with depth for soil at the Vaal River Mispah

Figure 6.6 pH in 0.1 M KCl results with depth for soil at the Vaal River Mispah

Figure 6.7 Conductivity results with depth for soil at the Vaal River West Complex

Figure 6.8 Conductivity results with depth for soil at the Vaal River Mispah

Figure 6.9 Redox potential results with depth for soil at the Vaal River West Complex

Figure 6.10 Redox potential results with depth for soil at the Vaal River Mispah

Figure 6.11 Moisture content results with depth for soil at the Vaal River West Complex

Figure 6.12 Moisture content results with depth for soil at the Vaal River Mispah

Figure 7.1 Results for cation exchange capacity with depth, for soil at the Vaal River West Complex

Figure 7.2 Results for cation exchange capacity with depth, for soil at the Vaal River Mispah

Figure 7.3 Results for variation of organic carbon with depth, for soil at the Vaal River West Complex

Figure 7.4 Results for variation of organic carbon with depth, for soil at the Vaal River Mispah

Figure 7.5 Results for phosphorous with depth, for soil at the Vaal River West Complex

Figure 7.6 Results for phosphorous with depth, for soil at the Vaal River Mispah

Figure 7.7 Results for potassium with depth, for soil at the Vaal River West Complex

Figure 7.8 Results for potassium with depth, for soil at the Vaal River Mispah

Figure 7.9 Results for nitrogen with depth, for soil at the Vaal River West Complex

Figure 7.10 Results for nitrogen with depth, for soil at the Vaal River Mispah

Figure 7.11 Results for calcium with depth, for soil at the Vaal River West Complex

Figure 7.12 Results for calcium with depth, for soil at the Vaal River Mispah

Figure 7.13 Results for magnesium with depth, for soil at the Vaal River West Complex

Figure 7.14 Results for magnesium with depth, for soil at the Vaal River Mispah

Figure 7.15 $\frac{10cm}{30cm}$ ratio curves for carbon, hydrogen, and nitrogen at the Vaal River West Complex

Figure 7.16 $\frac{10cm}{50cm}$ ratio curves for carbon, hydrogen, and nitrogen at the Vaal River Mispah

Figure 8.1 BCR sequential extraction curve with depth for calcium at the Vaal River West Complex

Figure 8.2 BCR sequential extraction curve with depth for calcium at the Vaal River Mispah

Figure 8.3 BCR sequential extraction curve with depth for magnesium at the Vaal River West Complex

Figure 8.4 BCR sequential extraction curve with depth for magnesium at the Vaal River Mispah

Figure 8.5 BCR sequential extraction curve with depth for phosphorous at the Vaal River West Complex

Figure 8.6 BCR sequential extraction curve with depth for phosphorous at the Vaal River Mispah

Figure 8.7 BCR sequential extraction curve with depth for potassium at the Vaal River West Complex

Figure 8.8 BCR sequential extraction curve with depth for potassium at the Vaal River Mispah

Figure 8.9 BCR sequential extraction curve with depth for sulphur at the Vaal River West Complex

Figure 8.10 BCR sequential extraction curve with depth for sulphur at the Vaal River Mispah

Figure 8.11 BCR sequential extraction curve with depth for aluminium at the Vaal River West Complex

Figure 8.12 BCR sequential extraction curve with depth for aluminium at the Vaal River Mispah

Figure 8.13 BCR sequential extraction curve with depth for arsenic at the Vaal River West Complex

Figure 8.14 BCR sequential extraction curve with depth for arsenic at the Vaal River Mispah

Figure 8.15 BCR sequential extraction curve with depth for chromium at the Vaal River West Complex

Figure 8.16 BCR sequential extraction curve with depth for chromium at the Vaal River Mispah

Figure 8.17 BCR sequential extraction curve with depth for copper at the Vaal River West Complex

Figure 8.18 BCR sequential extraction curve with depth for copper at the Vaal River Mispah

Figure 8.19 BCR sequential extraction curve with depth for iron at the Vaal River West Complex

Figure 8.20 BCR sequential extraction curve with depth for iron at the Vaal River Mispah

Figure 8.21 BCR sequential extraction curve with depth for lead at the Vaal River West Complex

Figure 8.22 BCR sequential extraction curve with depth for lead at the Vaal River Mispah

Figure 8.23 BCR sequential extraction curve with depth for manganese at the Vaal River West Complex

Figure 8.24 BCR sequential extraction curve with depth for manganese at the Vaal River Mispah

Figure 8.25 BCR sequential extraction curve with depth for mercury at the Vaal River West Complex

Figure 8.26 BCR sequential extraction curve with depth for mercury at the Vaal River Mispah

Figure 8.27 BCR sequential extraction curve with depth for nickel at the Vaal River West Complex

Figure 8.28 BCR sequential extraction curve with depth for nickel at the Vaal River Mispah

Figure 8.29 BCR sequential extraction curve with depth for titanium at the Vaal River West Complex

Figure 8.30 BCR sequential extraction curve with depth for titanium at the Vaal River Mispah

Figure 8.31 BCR sequential extraction curve with depth for uranium at the Vaal River West Complex

Figure 8.32 BCR sequential extraction curve with depth for uranium at the Vaal River Mispah

Figure 8.33 BCR sequential extraction curve with depth for vanadium at the Vaal River West Complex

Figure 8.34 BCR sequential extraction curve with depth for vanadium at the Vaal River Mispah

Figure 8.35 BCR sequential extraction curve with depth for zinc at the Vaal River West Complex

Figure 8.36 BCR sequential extraction curve with depth for zinc at the Vaal River Mispah

Figure 8.37 Elemental percentage distribution curves at the Vaal River West Complex for the control samples at 0-10 cm and 20-30 cm

Figure 8.38 Elemental percentage distribution curves at the Vaal River West Complex for *Rhus lancea* at 0-10 cm and 20-30 cm

Figure 8.39 Elemental percentage distribution curves at the Vaal River West Complex for *Tamarix usneoides* at 0-10 cm and 20-30 cm

Figure 8.40 Elemental percentage distribution curves at the Vaal River Mispah for the control samples at 0-10 cm and 40-50 cm

Figure 8.41 Elemental percentage distribution curves at the Vaal River Mispah for *Rhus lancea* at 0-10 cm and 40-50 cm

Figure 8.42 Elemental percentage distribution curves at the Vaal River Mispah for *Tamarix usneoides* at 0-10 cm and 40-50 cm

LIST OF TABLES

Table 5.1 The total number of soil core samples, i.e. control samples and tree samples, taken at the Vaal River sites

Table 5.2 The three stage BCR sequential extraction procedure extraction scheme (Rauret *et al.*, 2000)

Table 5.3 Typical soil fertility parameters, their range and ratings (FAO/IIASA/ISRIC/ISS-CAS/JRC, 2009; Yara Analytical Services, 2011; Mitchell *et al.*, 1995; Hill Laboratories, 2015; Coulter *et al.*, 2008; Espinoza *et al.*, 2006)

Table 5.4 Characterisation of the soil within each rating (FAO/IIASA/ISRIC/ISS-CAS/JRC, 2009; Yara Analytical Services, 2011; Mitchell *et al.*, 1995)

Table 5.5 The NCS DC 73315 certified elemental totals reference values versus the experimental values

Table 5.6 The NCS DS 73315 certified elemental concentrations versus the experimental values

Table 5.7 The BCR 701 CRM certified reference values compared to experimental values

Table 6.1 Descriptive statistics of initial soil solution measurements by site

Table 6.2 Descriptive statistics of initial soil solution measurements by treatment

Table 6.3 Descriptive statistics of initial soil solution measurements by type of tree

Table 6.4(a) Descriptive statistics of initial soil solution measurements; soil pH and pH in KCl by depth

Table 6.4(b) Descriptive statistics of initial soil solution measurements; conductivity, redox potential and moisture content by depth

Table 6.5 The PCA of the initial soil solution measurements

Table 7.1 Changes in soil texture and bulk density values with depth for soil at the Vaal River West Complex

Table 7.2 Changes in soil texture and bulk density values with depth for soil at the Vaal River Mispah

Table 7.3 Descriptive statistics of soil texture measurements by site

Table 7.4 Descriptive statistics of soil texture measurements by treatment

Table 7.5 Descriptive statistics of soil texture measurements by type of tree

Table 7.6 Descriptive statistics of soil texture measurements by site and depth

Table 7.7 The PCA of the soil texture analysis

Table 7.8 Descriptive statistics of soil fertility measurements by site

Table 7.9 Descriptive statistics of soil fertility measurements by treatment

Table 7.10 Descriptive statistics of soil fertility measurements by type of tree

Table 7.11 Descriptive statistics of soil fertility measurements by site and depth

Table 7.12 The PCA of the soil fertility measurements

Table 7.13 Descriptive statistics of CHNS data by site

Table 7.14 Descriptive statistics of CHNS data by treatment

Table 7.15 Descriptive statistics of CHNS data by type of tree

Table 7.16(a) Descriptive statistics of carbon and hydrogen data by site and depth

Table 7.16(b) Descriptive statistics of nitrogen data by site and depth

Table 7.17 The PCA of the CHNS data

Table 8.1 Descriptive statistics of major nutrients by site

Table 8.2 Descriptive statistics of major nutrients by treatment

Table 8.3 Descriptive statistics of major nutrients by type of tree

Table 8.4 Descriptive statistics of major nutrients by sequential extraction step

Table 8.5(a) Descriptive statistics of the major nutrients, calcium, magnesium and phosphorous, by site and depth

Table 8.5(b) Descriptive statistics of the major nutrients, potassium and sulphur by site and depth

Table 8.6 The PCA of the major nutrients

Table 8.7 A summary of the one-way ANOVA results for the components of the major nutrients

Table 8.8 A summary of the LRA for the components of the major nutrients

Table 8.9 Descriptive statistics of trace elements by site

Table 8.10 Descriptive statistics of trace elements by treatment

Table 8.11 Descriptive statistics of trace elements by type of tree

Table 8.12 Descriptive statistics of trace elements by sequential extraction step

Table 8.13(a) Descriptive statistics of aluminium, arsenic, chromium, copper, and iron by site and depth

Table 8.13(b) Descriptive statistics of lead, manganese, mercury, nickel, and titanium by site and depth

Table 8.13(c) Descriptive statistics of uranium, vanadium and zinc by site and depth

Table 8.14 The PCA of the trace elements

Table 8.15 A summary of the one-way ANOVA results for the components of the trace elements

Table 8.16 A summary of the LRA for the components of the trace elements

LIST OF ABBREVIATIONS

AGA	AngloGold Ashanti Ltd
AMD	Acid mine drainage
ANOVA	Analysis of Variance
ARD	Acid rock drainage
BCR	European Community Bureau of Reference
CCD	Charge coupled detector
CEC	Cation exchange capacity
Cedara	KwaZulu-Natal Department of Agriculture and Environmental Affairs
CHNS	Carbon, hydrogen, nitrogen and sulphur elemental analysis
CRM	Certified reference material
CT	Control
ECEC	Effective cation exchange capacity
ICP-OES	Inductively coupled plasma – Optical emission spectroscopy
NEMA	National Environmental Management Act
PCA	Principal components analysis
PVC	Poly vinyl chloride
RL	*Rhus lancea*
SPSS	Statistical Package for Social Sciences
TSF	Tailings storage facility
TX	*Tamarix usneoides*
VRMP	Vaal River Mispah

VRWC	Vaal River West Complex
XRF	X-Ray fluorescence spectroscopy

LIST OF SYMBOLS

%	percentage
µm	micrometre
µS cm^{-1}	micro-Siemens per centimetre
°C	degrees Celsius
cm	centimetre
cmol kg^{-1}	centi-mole per kilogram
Eh	redox potential
g cm^{-3}	grams per cubic centimetre
g	gram
K	kelvin
km	kilometre
km^2	kilometres squared
m	metre
M	molarity, moles per litre
mg kg^{-1}	milligrams per kilogram
mg L^{-1}	milligram per litre
mL	millilitre
mm	millimetre
mm	millimetre
mol L^{-1}	moles per litre
V	volt

ppm	parts per million
US$	US dollars